

## Synthesis of MnO<sub>2</sub> as Supercapacitor Electrodes Material by Green Chemistry Method Through Dihydroxylation of Tangerine Peel (*Citrus reticulata*) Essential Oil

Dewi Jalinan Izzah<sup>\*</sup>, Fauziatul Fajarah, Adilah Aliyatulmuna, Sumari Sumari, Siti Marfu'ah

Department of Chemistry, Faculty of Mathematics and Science, The State University of Malang, Jl. Semarang 5, Malang City, Indonesia

<sup>\*</sup>Corresponding Author: [dewijalinanizzah@gmail.com](mailto:dewijalinanizzah@gmail.com)

Received: August,22,2022 /Accepted: December,23,2022

doi: 10.24252/al-kimiav10i2.31459

**Abstract:** In this digital era, most technology requires electronic equipment. The performance of electronic equipment may be affected by energy storage components like a supercapacitor, so the development of supercapacitor electrode materials using green chemical methods needs to be pursued. Material with a good specific capacitance is MnO<sub>2</sub>. Most of the MnO<sub>2</sub> synthesis methods are not based on green chemistry, so there is an alternative method. One of them is by utilizing the waste from tangerine peels. This study aimed to synthesize MnO<sub>2</sub> through dihydroxylation of tangerine peel essential oil. The steps for conducting this research consisted of isolation of tangerine peel essential oil, analysis of the constituent components of tangerine peel essential oil, synthesis of MnO<sub>2</sub> through dihydroxylation of essential oils tangerine peel, and MnO<sub>2</sub> characterization. XRD results showed that MnO<sub>2</sub> synthesized at pH 11 had the highest percentage of  $\alpha$ -MnO<sub>2</sub> (97%). This is evidenced by the presence of  $\alpha$ -MnO<sub>2</sub> diffractogram according to the ICSD No.20227. The SEM results showed that MnO<sub>2</sub> had a spherical morphology with a particle diameter of 39.51 nm.  $\alpha$ -MnO<sub>2</sub> has a larger tunnel structure compared to  $\beta$ - and  $\gamma$ -MnO<sub>2</sub>, making the charge-discharge process easier so that  $\alpha$ -MnO<sub>2</sub> has the potential as a supercapacitor electrode material.

**Key word:** Tangerine peel essential oil, green chemistry, MnO<sub>2</sub>, electrode, supercapacitor

### INTRODUCTION

Energy needs in this digital era are increasing, so scientists in the world are developing various technologies, including energy storage components. This shows that technology is progressing so that it causes the importance of energy needs in high quantities. Electric vehicles, *gadgets*, and laptops include electronic equipment that requires energy storage components such as lithium-ion batteries. Lithium-ion batteries have the disadvantage of having a low density (<1 kW.kg<sup>-1</sup>) and short cycle life. Supercapacitors can be an alternative to lithium-ion batteries because they have a high density (>1 kW.kg<sup>-1</sup>) and long cycle life (F. Zhang et al., 2013). Supercapacitors are components that function to store electric charge high specific (Conway, 1999). To support the function of the supercapacitor, an electrode is needed as a primary component. Materials that have been used as supercapacitor electrode materials are MnO<sub>2</sub> (Wang, 2016), Co<sub>3</sub>O<sub>4</sub> (Samal et al., 2017), RGO (Bhujel et al., 2019), NiCo<sub>2</sub>O<sub>4</sub> (Ko et al., 2017), and RuO<sub>2</sub> (Thangappan et al., 2018). MnO<sub>2</sub> was chosen as the supercapacitor electrode material in this study because of its low toxicity, environmental friendliness, and high specific capacity (1370 Fg<sup>-1</sup>) (Wang, 2016) compared to Co<sub>3</sub>O<sub>4</sub> (833 Fg<sup>-1</sup>) (Samal et al., 2017), RGO (50 Fg<sup>-1</sup>) (Bhujel et al., 2019), NiCo<sub>2</sub>O<sub>4</sub> (886 Fg<sup>-1</sup>) (Ko et al., 2017), and RuO<sub>2</sub> (441.1 Fg<sup>-1</sup>) (Thangappan et al., 2018).

The most of the reductants used to synthesize MnO<sub>2</sub> are materials that are not environmentally friendly, such as Mn(CH<sub>3</sub>CO<sub>2</sub>)<sub>2</sub> (Kahattha & Santhaveesuk, 2019), MnCl<sub>2</sub> (Kolkovskiy et al., 2020), and HCl (Balakumar et al., 2020). So it is necessary to do research on the synthesis of MnO<sub>2</sub> through green chemical methods, namely utilizing environmentally friendly organic waste such as lemon peel (Hashem et al., 2018), apple peel (Sanchez-Botero et al., 2017), and cabbage leaves (Chatterjee et al., 2017). So far, research on the synthesis of MnO<sub>2</sub> using essential oils from natural ingredients has not been developed optimally and effectively, so in this study, tangerine peel essential oil will be used as a reducing agent.

Tangerine peel essential oil was isolated using steam-water distillation. This type of technique was chosen because, during the refining process, the tangerine peel does not come into direct contact with a heat source that can damage the components of the compound in the material. In addition, this technique is more efficient and simpler than steam distillation and water distillation (Katiyar, 2017). Based on the results of GC-MS analysis from previous studies, tangerine peel essential oil mostly contains alkene components in the form of limonene (97.688%) (Ngo et al., 2020). The abundance of limonene in tangerine peel essential oil has the potential as a reducing agent in the synthesis of MnO<sub>2</sub> through dihydroxylation of alkenes to reduce Mn(VII) in KMnO<sub>4</sub> to Mn(IV). Based on the explanation above, this research was carried out with the aims of: 1) Producing MnO<sub>2</sub> from KMnO<sub>4</sub> through the dihydroxylation reaction of alkene components of tangerine peel essential oil in an alkaline environment and 2) Knowing the crystallinity and morphology of the synthesized MnO<sub>2</sub>.

## RESEARCH METHODS

### Materials and Tools

The materials used in this research were fresh tangerine peel from Gadingkulon Village, KMnO<sub>4</sub> p.a (merck), KOH p.a (merck), n-hexane, and demineralized aqua (Hydrobatt). The tools used in this research is a set of steam-water distillation apparatus, pH meter (WTW pH 3110), manual balance (to 0.1), analytical balance (Shimadzu to 0.0001 g), pycnometer (IWAKI 5 mL), ultrasonic bath (Branson 1510), centrifuge (Kokusan, type H-103n), oven (Mettler, type UN 55), furnace (Nabertherm), GC-MS (Agilent, types 7890B and 5977B), XRD ( Rigaku MiniFlex), and SEM (FEI, Inspect-S50 type).

### Methods

#### *Isolation of Tangerine Peel Essential Oil Using Steam-Water Distillation*

The fresh tangerine peels were cleaned of impurities and cut into small pieces. Then aerated for 3 days until the tangerine peel wilts. Then weighed as much as 1-2 kg. The wilted tangerine peel was put into a distillation boiler filled with water below its sieve. After that, the distillation boiler was closed, then connected to a condenser, hose, adapter, and container bottle. The distillation boiler was heated on the stove for eight hours. After that, the essential oil is separated from the water using a dry and clean pipette dropper. The mass of essential oils is weighed, then the yield is calculated using equation:

$$\% \text{Yield} = \frac{\text{Tangerine peel essential oil mass}}{\text{Wilted tangerine peel mass}} \times 100 \quad (\text{Eq.1})$$

***Analysis of the Components of Tangerine Peel Essential Oils Using GC-MS***

Analysis of the components of tangerine peel essential oil was carried out using the Gas Chromatography-Mass Spectrometer (GC-MS) instrument at the Forensic Laboratory Center of the National Police Criminal Investigation Agency, Bogor. Based on the results of GC analysis, is known the number of components that make up the essential oil through the number of peaks on the chromatogram. Based on the results of MS analysis, it is known the types of compounds contained in essential oils through the fragmentation of molecular ions.

***Synthesis of MnO<sub>2</sub> Through Dihydroxylation Reaction of Tangerine Peel Essential Oil***

The MnO<sub>2</sub> synthesis process is based on research conducted by Badriawati, AT (2021) and Mahmudi et al. (2018) modified. A solution of 30 mL of 0.5 M KMnO<sub>4</sub> was mixed with 2 mL of tangerine peel essential oil. Added dropwise 0.5 M KOH solution. The mixture has flowed with ultrasonic waves at a frequency of 40 kHz and a temperature of 27°C. The pH of the mixture was measured. This procedure was repeated three times to obtain different alkaline pH data. This reaction produces a dark brown precipitate. The precipitate was separated from the solution using a centrifuge at 1500 rpm for 10 minutes. After that, the MnO<sub>2</sub> was washed using n-hexane to dissolve the organic compounds. Then, the MnO<sub>2</sub> was washed with demineralized water to dissolve other impurities. Finally, the MnO<sub>2</sub> was calcined using a furnace at a temperature of 500°C for four hours (Kahattha & Santhaveesuk, 2019).

***MnO<sub>2</sub> Characterization***

The MnO<sub>2</sub> was characterized by using X-Ray Diffraction (XRD) at Glabs Indonesia. To determine the type of MnO<sub>2</sub>, qualitative and quantitative diffractogram analysis was carried out. Qualitative analysis by matching the diffractogram data with ICSD data to analyze the expected suitability of the material. Quantitative analysis was carried out by analyzing the percent purity and lattice parameters of the synthesized MnO<sub>2</sub> through calculations using QualX and MAUD software. After confirming that MnO<sub>2</sub> was successfully formed, a Scanning Electron Microscope (SEM) test was carried out at the Mineral and Advanced Materials Laboratory, Department of Chemistry, FMIPA UM. The results of the SEM test were analyzed for morphology using ImageJ and Origin9 software.

**RESULTS AND DISCUSSION****Results of Essential Oil Isolation**

The isolation process was carried out using low heat so that the distillate that comes out of the condenser is not hot, it does not evaporate easily. Calculation of the yield of tangerine peel essential oil was carried out using Eq.1. The data obtained from the distillation of tangerine peels are shown in Table 1.

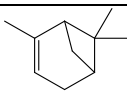
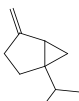
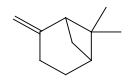
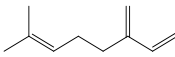
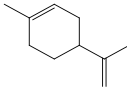
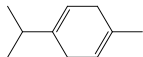
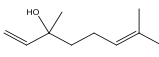
**Table 1.** Data on the steam-water distillation of tangerine peels

Distillation to-	Withered Tangerine Peel Mass (g)	Essential Oil Volume (mL)	Essential Oil Density (g/mL)	Mass of Essential Oil (g)	Yield (%)
1	1035	18.5	0.88452	16.4895	1,593
2	2022	20	0.88494	18,5040	0.915

Tangerine peel essential oil was then analyzed using the GC-MS instrument to determine the types of compounds contained in it, so that it can be ascertained that the tangerine peel essential oil could be used as a reducing agent in the synthesis of MnO<sub>2</sub>. The percentages of compound abundance and their retention times are shown in Table 2.

This data shows that the tangerine peel essential oil is mostly composed of components of unsaturated hydrocarbon compounds with the largest abundance being limonene compounds (71.18%). These results are following the research conducted by Devi, P. L. (2021), that the largest component in the essential oil of tangerine peel isolated using steam-water distillation is limonene compound (26.16%). This difference in limonene content is due to different agricultural systems and soil fertility conditions (Anita, 2012).

**Table 2.** Compound components in tangerine peel essential oil

No.	Compound Name	Retention Time (min.)	Abundance (%)	m/z	Structure
1.	$\alpha$ -pinene	4.452	1.42	136	
2.	sabinene	4.983	1.28	136	
3.	$\beta$ -pinene	5.050	5.31	136	
4.	$\beta$ -myrcene	5.180	3.56	136	
5.	limonene	5.833	71.18	136	
6.	$\gamma$ -terpinene	6.192	2.19	136	
7.	linalool	6.749	5.13	154	
8.	Other compounds (9.93%)				

### Results of MnO<sub>2</sub> Synthesis

Based on the data from the GC-MS analysis shown in Table 2, tangerine peel essential oil is mostly composed of components of alkene compounds, so this material can be used as a reducing agent for KMnO<sub>4</sub> through a dihydroxylation reaction of alkenes under alkaline conditions with the help of ultrasonic waves to produce MnO<sub>2</sub>. The MnO<sub>4</sub><sup>-</sup> ion is a strong oxidizing agent with an oxidation number of manganese +7 (Rayner, G. & Overton, 2014). The Mn(+7) ion was reduced to Mn(+4) by using tangerine peel essential oil through a dihydroxylation reaction of alkene to form a diol compound and a black solid which was suspected to be MnO<sub>2</sub>. This reaction is initiated by the nucleophilic attack of MnO<sub>4</sub><sup>-</sup> on the carbon atom of the alkene so that the pi ( $\pi$ ) bond in the alkene is broken. The three electron pairs of the alkene and MnO<sub>4</sub><sup>-</sup> are delocalized to form a new sigma ( $\sigma$ ) bond. Then a cyclic intermediate Mn(+5) diester is formed. Furthermore, there is a nucleophilic attack from the hydroxyl ion on the intermediate, so the Mn-O bond is broken and produces diol and MnO<sub>2</sub> compounds (Figure 1).

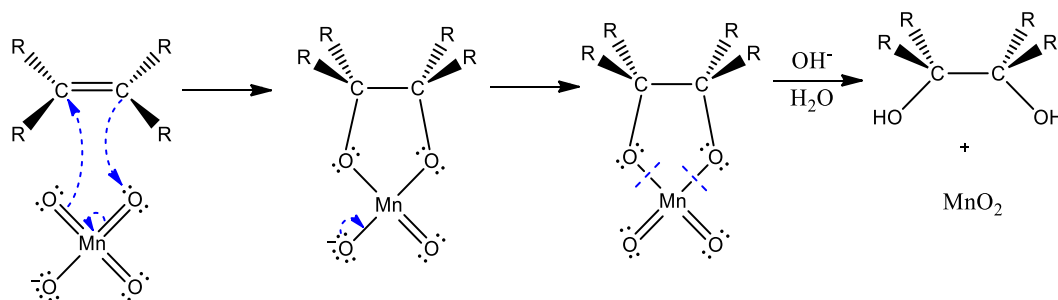


Figure 1. Alkene dihydroxylation reaction mechanism (Marfu'ah, 2014)

Data observed during the synthesis of MnO<sub>2</sub> are shown in Table 3. KMnO<sub>4</sub> as precursor dissolved in water produces a purple solution. Then 2 mL of essential oil was added to the KMnO<sub>4</sub> solution to reduce Mn(+7) ions to Mn(+4). Add 0.5 M KOH solution dropwise to adjust the pH of the mixture. In this process, the alkene syn addition dihydroxylation reaction occurs, namely the double bond in limonene is added by two hydroxyl groups originating from basic KMnO<sub>4</sub> solution, resulting in ethane-1,2-diol with two hydroxyl groups facing each other. The mixture was given ultrasonic waves at a frequency of 40 kHz and a temperature of 27°C, resulting in a blackish brown precipitate which was estimated to be MnO<sub>2</sub>. The sonochemical method is effective because the reaction can be regulated at a relatively low temperature, 27°C (Abulizi et al., 2014). This method also involves the formation and explosion of bubbles in the mixture accompanied by rapid cooling, so that nano-sized particles will be formed (Patil & Bhanage, 2016). Then the pH of the mixture was measured using a pH meter. After that, centrifugation was carried out for 10 minutes at a speed of 1500 rpm to separate the precipitate and solution. This procedure was repeated three times to obtain a pH of 9.1; 9.8; and 11. The variation of the pH of this mixture aims to determine the effect of the pH of the mixture on the crystallinity of the MnO<sub>2</sub> formed. The observed data when synthesizing MnO<sub>2</sub> are presented in Table 3.

Table 3. Observational data during the synthesis of MnO<sub>2</sub>

Observed Object	Observation result
<b>Before reaction</b>	
Tangerine peel essential oil color	Clear yellow
Color of KmnO <sub>4</sub> solution 0.5 M	Purple
Color of 0.5 M KOH solution	Colorless
<b>After reaction</b>	
The pH of mixture 1	9.1
The pH of mixture 2	9.8
The pH of mixture 3	11
Mass of MnO <sub>2</sub> from pH 9.1	1.5646 grams
Mass of MnO <sub>2</sub> from pH 9.8	1.3931 grams
Mass of MnO <sub>2</sub> from pH 11	1.5525 grams
Solid color	Black

The solid sample suspected to be MnO<sub>2</sub> was characterized by using X-Ray Diffraction (XRD) to confirm the success of the synthesis, resulting in a diffractogram. Then the analysis is carried out by comparing the experimental diffractogram data with the standard diffractogram data in ICSD (*Inorganic Crystal Structure Database*) to determine the expected suitability of the material. The diffractogram of XRD test results on MnO<sub>2</sub> synthesized at different pH conditions produced several peaks as shown in Figure 2. This shows that pH can affect the formation of several polymorphs in MnO<sub>2</sub> (Zhao et al., 2017).

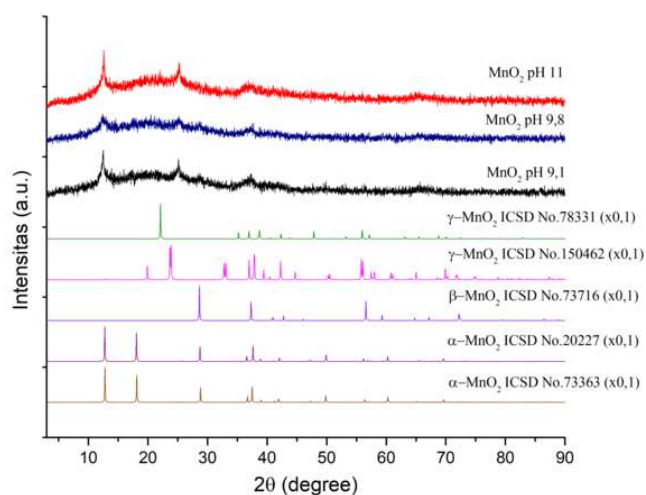


**Figure 2.** The diffractogram of synthesized MnO<sub>2</sub> at pH 9.1, 9.8, and 11

It can be observed that the sharp peaks in the diffractogram of the synthesized MnO<sub>2</sub> correspond to the standard pattern from ICSD, so it is known that the synthesized MnO<sub>2</sub> has three kinds of polymorphs ( $\alpha$ ,  $\beta$ ,  $\gamma$ ). The crystal lattice structure of each synthesized MnO<sub>2</sub> polymorph is shown in Figure 3.

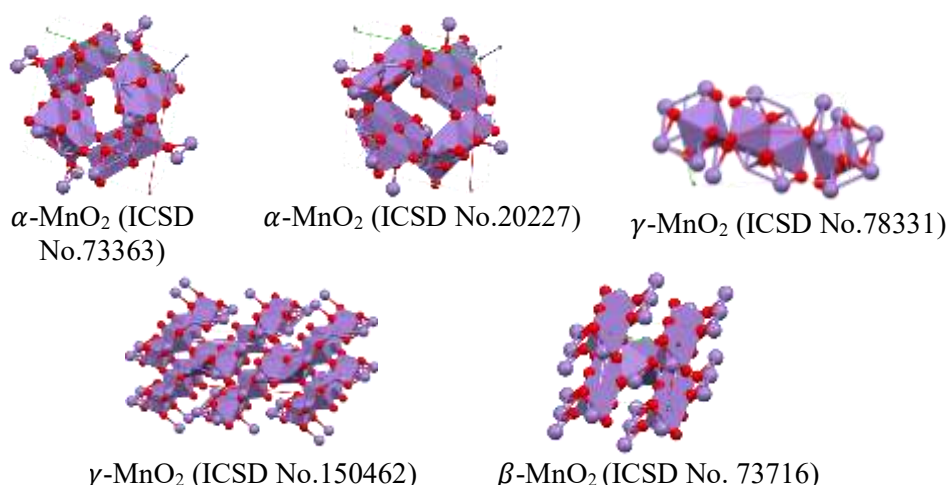


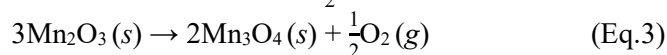
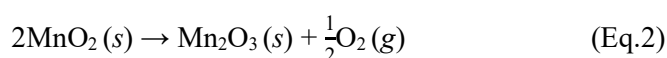
**Figure 3.** Crystal lattice structure of  $\alpha$ -,  $\beta$ -, and  $\gamma$ -MnO<sub>2</sub>

To determine the percentage of MnO<sub>2</sub> contained in the sample, the MAUD software was used. Table 5 shows the percentage and crystallographic data of MnO<sub>2</sub>. MnO<sub>2</sub> synthesized at pH 11 had a polymorphic percentage  $\alpha$  the largest (97.16%) compared to MnO<sub>2</sub> treated synthesis at pH 9.1 and pH 9.8.

**Table 5.** Percentages and crystallographic data of the synthesized compounds

Compound Name	Percentage (%)	Crystal Grid	Grid Angle (°)	Grid Length (Å)
<b>pH 9.1</b>				
$\alpha$ -MnO <sub>2</sub> -1 (ICSD No.73363)	29.334465±0.0	Tetragonal	$\alpha=90; \beta=90; \gamma=90$	$a=9.7876; b=9.7876; c=2.8650$
$\gamma$ -MnO <sub>2</sub> -1 (ICSD No. 150462)	28.049166±8.53899	Monoclinic	$\alpha=90; \beta=90.5; \gamma=90$	$a=13.7; b=2.867; c=4.46$
$\beta$ -MnO <sub>2</sub> _ (ICSD No.73716)	47.619476±1237.7917	Tetragonal	$\alpha=90; \beta=90; \gamma=90$	$a=4.4041; b=4.4041; c=2.8765$
Mn <sub>3</sub> O <sub>4</sub> -1 (ICSD No. 40110)	2.4086256±64.35247	Orthorhombic	$\alpha=90; \beta=90; \gamma=90$	$a=9.5564; b=9.7996; c=3.0240$
<b>pH 9.8</b>				
$\alpha$ -MnO <sub>2</sub> -2 (ICSD No. 20227)	7.1243024±0.0	Tetragonal	$\alpha=90; \beta=90; \gamma=90$	$a=9.815; b=9.815; c=2.847$
$\gamma$ -MnO <sub>2</sub> -2 (ICSD No. 78331)	92.46286 ±1226.0414	Orthorhombic	$\alpha=90; \beta=90; \gamma=90$	$a=9.229; b=4.4533; c=2.8482$
Mn <sub>3</sub> O <sub>4</sub> -1 (ICSD No. 40110)	0.41283733±0.7823502	Orthorhombic	$\alpha=90; \beta=90; \gamma=90$	$a=9.5564; b=9.7996; c=3.0240$
<b>pH 11</b>				
$\alpha$ -MnO <sub>2</sub> -2 (ICSD No. 20227)	97.158295±4332.6636	Tetragonal	$\alpha=90; \beta=90; \gamma=90$	$a=9.815; b=9.815; c=2.847$
$\gamma$ -MnO <sub>2</sub> -2 (ICSD No. 78331)	0.17742667 ±12.5603	Orthorhombic	$\alpha=90; \beta=90; \gamma=90$	$a=9.3229; b=4.4533; c=2.8482$
Mn <sub>3</sub> O <sub>4</sub> -1 (ICSD No. 40110)	1.7380179 ±71.66481	Orthorhombic	$\alpha=90; \beta=90; \gamma=90$	$a=9.5564; b=9.7996; c=3.0240$
Mn <sub>3</sub> O <sub>4</sub> -2 (ICSD No. 30005)	0.92626035±37.417515	Orthorhombic	$\alpha=90; \beta=90; \gamma=90$	$a=3.026; b=9.769; c=9.568$

The large percentage of  $\alpha$ -MnO<sub>2</sub> synthesized at pH 11 has the potential to be used as a supercapacitor electrode material. Because  $\alpha$ -MnO<sub>2</sub> has a tunnel structure (2 x 2) measuring about 4.6 x 4.6 so that cations can be intercalated into the tunnel during the charge-discharge cycle process that occurs in the supercapacitor, compared to other polymorphs such as  $\beta$  (1 x 1) and  $\gamma$  ((1 x 1)/(1 x 2)) which have a narrow tunnel size (Zhao et al., 2017). In addition, at pH 11 an impurity in the form of Mn<sub>3</sub>O<sub>4</sub> was produced with the smallest percentage of 2.66%. Mn<sub>3</sub>O<sub>4</sub> is probably formed due to the heating of MnO<sub>2</sub> at high temperatures (~above 400°C) resulting in the release of oxygen. The process of formation of Mn<sub>3</sub>O<sub>4</sub> follows the following reaction equation (H. Zhang et al., 2014). Therefore, the type of crystal chosen as the supercapacitor electrode material is  $\alpha$ -MnO<sub>2</sub>.



After confirming that MnO<sub>2</sub> was successfully formed, a Scanning Electron Microscope (SEM) test was carried out to determine the morphological structure of the synthesized MnO<sub>2</sub>. The results of the SEM analysis with a magnification of 20,000 times are shown in Figure 4 below. At pH 9.1; 9.8; and 11 formed MnO<sub>2</sub> with spherical morphology and agglomeration occurred.

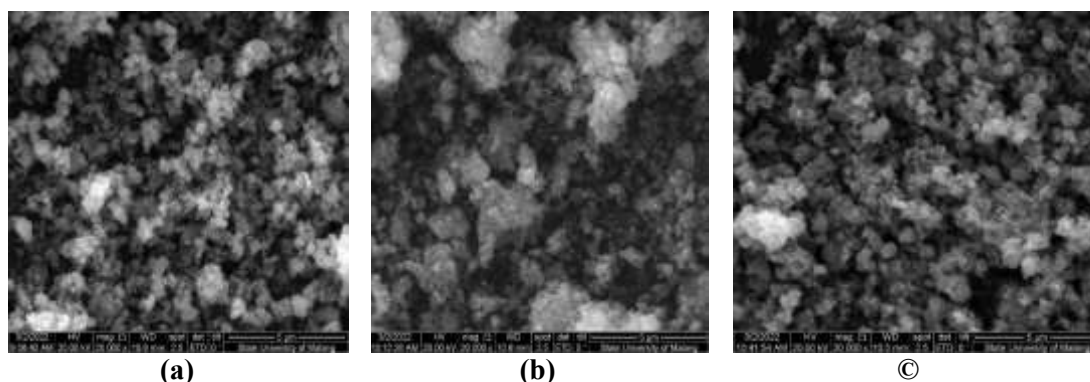


Figure 6. Morphology of synthesized MnO<sub>2</sub> at pH: a) 9.1; b) 9.8; and c) 11

To determine the particle size of the synthesized MnO<sub>2</sub>, an analysis was carried out using ImageJ and Origin software, to obtain the data shown in Table 6. From these data, it can be proven that the MnO<sub>2</sub> synthesized includes nanoparticles. Because material is called a nanoparticle if it has an average particle size of 10-100 nm (Tiloke et al., 2016).

pH conditions for the synthesis of MnO <sub>2</sub>	Average MnO <sub>2</sub> particle size (nm)
9.1	66.87
9.8	54.88
11	39.51

Table 6 shows that the difference in pH of the mixture can affect the particle size of MnO<sub>2</sub> (Abulizi et al., 2014). Thus, the optimal pH for synthesizing MnO<sub>2</sub> is 11. Because at pH 11, the smallest MnO<sub>2</sub> particles are produced, and the highest percentage of  $\alpha$ -MnO<sub>2</sub> is produced.

## CONCLUSIONS

MnO<sub>2</sub> was successfully synthesized using the green chemical method by hydroxylation of alkenes with tangerine peel essential oil as a reducing agent, which mostly contained a limonene component of 71.18%. XRD test results showed that the MnO<sub>2</sub> synthesized at pH 11 had the highest percentage of  $\alpha$ -MnO<sub>2</sub> (97 %). SEM test results showed that MnO<sub>2</sub> synthesized at pH 11 had a spherical morphology but agglomerated with an average particle diameter of 39.51 nm.  $\alpha$ -MnO<sub>2</sub> has a tunnel structure (2 x 2) which is larger in size than  $\beta$ - and  $\gamma$ -MnO<sub>2</sub>. This makes it easier for the charge-discharge process, so that  $\alpha$ -MnO<sub>2</sub> has the potential as a supercapacitor electrode material.



## REFERENCES

- Abulizi, A., Yang, G. H., Okitsu, K., & Zhu, J.-J. 2014. Synthesis of MnO<sub>2</sub> nanoparticles from sonochemical reduction of MnO<sub>4</sub><sup>-</sup> in water under different pH conditions. *Ultrasonics Sonochemistry*, 21(5), 1629–1634. <https://doi.org/10.1016/j.ultsonch.2014.03.030>
- Anita, P. D. 2012 . Kandungan Vitamin C Buah dan Komponen Minyak Atsiri Kulit Buah Jeruk Keprok (*Citrus nobilis*) pada Ketinggian yang Berbeda di Lereng Gunung Lawu. Universitas Sebelas Maret.
- Badriawati, A. T. 2021 . Sintesis MnO<sub>2</sub> Sebagai Kandidat Elektroda Superkapasitor Kinerja Tinggi dengan Metode Kimia Hijau Melalui Dihidroksilasi Minyak Atsiri Kulit Jeruk Baby (*Citrus sinensis*).
- Balakumar, V., Ryu, J. W., Kim, H., Manivannan, R., & Son, Y. A. 2020 . Ultrasonic Synthesis of  $\alpha$ -MnO<sub>2</sub> Nanorods: An Efficient Catalytic Conversion of Refractory Pollutant, Methylene Blue. *Ultrasonics Sonochemistry*, 62, 104870. <https://doi.org/10.1016/j.ultsonch.2019.104870>
- Bhujel, R., Rai, S., Deka, U., & Swain, B. P. 2019. Electrochemical, Bonding Network and Electrical Properties of Reduced Graphene Oxide-Fe<sub>2</sub>O<sub>3</sub> Nanocomposite for Supercapacitor Electrodes Applications. *Journal of Alloys and Compounds*, 792, 250–259. <https://doi.org/10.1016/J.JALLCOM.2019.04.004>
- Chatterjee, S., Ja, A., Subramanian, A., & Subramanian, S. 2017 . Synthesis and Characterization of Manganese Dioxide Using *Brassica oleracea* (Cabbage). *Journal of Industrial Pollution Control*, 33(2), 1627–1632.
- Conway, B. E. 1999 . Electrochemical Supercapacitors: Scientific Fundamentals and Technological Applications. Kluwer Academic / Plenum Publishers.
- Devi, P. L. 2021 . Komponen Kimia dan Aktivitas Biologi Minyak Atsiri dari Kulit Jeruk Keprok (*Citrus reticulata*) yang diisolasi dengan Distilasi Uap Air dan Maserasi n-Heksana. <http://repo.undiksha.ac.id/id/eprint/7140>
- Hashem, A. M., Abuzeid, H., Kaus, M., Indris, S., Ehrenberg, H., Mauger, A., & Julien, C. M. 2018 . Green Synthesis of Nanosized Manganese Dioxide as Positive Electrode for Lithium-Ion Batteries Using Lemon Juice and Citrus Peel. *Electrochimica Acta*, 262, 74–81. <https://doi.org/10.1016/j.electacta.2018.01.024>
- Kahattha, C., & Santhaveesuk, S. 2019 . Influence of Calcination Temperature on Physical and Electrochemical Properties of MnO<sub>2</sub> Nanoparticles Synthesized by Co-Precipitation Method. *Ferroelectrics*, 552(1), 121–131. <https://doi.org/10.1080/00150193.2019.1653088>
- Katiyar, R. 2017 . Modeling and Simulation of *Mentha arvensis L.* Essential Oil Extraction by Water-Steam Distillation Process. *International Research Journal of Engineering and Technology (IRJET)*, 4(6), 2793–2798. <https://irjet.net/archives/V4/i6/IRJET-V4I6693.pdf>

- Ko, T. H., Radhakrishnan, S., Seo, M. K., Khil, M. S., Kim, H. Y., & Kim, B. S. 2017 . A Green and Scalable Dry Synthesis of NiCo<sub>2</sub>O<sub>4</sub>/Graphene Nanohybrids for High-Performance Supercapacitor and Enzymeless Glucose Biosensor Applications. *Journal of Alloys and Compounds*, 696, 193–200. <https://doi.org/10.1016/J.JALLCOM.2016.11.234>
- Kolkovskiy, P. I., Rachiy, B. I., Kolkovskiy, M. I., Ostafiychuk, B. K., Yaremiy, I. P., Kotsyubynsky, V. O., & Ilitsky, R. V. 2020 . Synthesis and Electrochemical Properties of Mesoporous  $\alpha$ -MnO<sub>2</sub> for Supercapacitor Applications. *Journal of Nano- and Electronic Physics*, 12(3), 03030-1-03030–03034. [https://doi.org/10.21272/jnep.12\(3\).03030](https://doi.org/10.21272/jnep.12(3).03030)
- Mahmudi, Widiyastuti, Nurlilasari, P., Affandi, S., and Setyawan, H. 2018 . Manganese Dioxide Nanoparticles Synthesized by Electrochemical Method and Its Catalytic Activity Towards Oxygen Reduction Reaction. *Journal of the Ceramic Society of Japan*, 11(126), 906–913. <https://doi.org/http://doi.org/10.2109/jcersj2.18091>
- Marfu'ah, S. 2014. *Mekanisme Reaksi-Reaksi Organik*. Universitas Negeri Malang.
- Ngo, T. C. Q., Tran, T. K. N., Nguyen, V. M., & Mai, H. C. 2020 . Optimization of Green Mandarin (*Citrus reticulata*) Essential Oil Extraction Using Microwave-Assisted Hydrodistillation and Chemical Composition Analysis. *IOP Conference Series: Materials Science and Engineering*, 991(1). <https://doi.org/10.1088/1757-899X/991/1/012122>
- Patil, A. B., & Bhanage, B. M. 2016 . Sonochemistry: A Greener Protocol for Nanoparticles Synthesis. *Handbook of Nanoparticles*, 143–166. [https://doi.org/10.1007/978-3-319-15338-4\\_4](https://doi.org/10.1007/978-3-319-15338-4_4)
- Rayner, G. & Overton, C. T. 2014 . Descriptive Inorganic Chemistry Sixth Edition. In *W. H. Freeman and Company* (Sixth). W. H. Freeman and Company. [www.ehfreeman.com](http://www.ehfreeman.com)
- Samal, R., Dash, B., Sarangi, C. K., Sanjay, K., Subbaiah, T., Senanayake, G., & Minakshi, M. 2017 . Influence of Synthesis Temperature on The Growth and Surface Morphology of Co<sub>3</sub>O<sub>4</sub> Nanocubes For Supercapacitor Applications. *Nanomaterials*, 7(11). <https://doi.org/10.3390/nano7110356>
- Sanchez-Botero, L., Herrera, A. P., & Hinestroza, J. P. 2017 . Oriented Growth of  $\alpha$ -MnO<sub>2</sub> Nanorods Using Natural Extracts from Grape Stems and Apple Peels. *Nanomaterials* 2017, Vol. 7, Page 117, 7(5), 117. <https://doi.org/10.3390/NANO7050117>
- Thangappan, R., Arivanandhan, M., Dhinesh Kumar, R., & Jayavel, R. 2018 . Facile Synthesis of RuO<sub>2</sub> Nanoparticles Anchored on Graphene Nanosheets for High Performance Composite Electrode for Supercapacitor Applications. *Journal of Physics and Chemistry of Solids*, 121, 339–349. <https://doi.org/10.1016/j.jpics.2018.05.049>

- Tiloke, C., Phulukdaree, A., & Chuturgoon, A. A. 2016 . The Chemotherapeutic Potential of Gold Nanoparticles Against Human Carcinomas: A Review. *Nanoarchitectonics for Smart Delivery and Drug Targeting*, 783–811. <https://doi.org/10.1016/B978-0-323-47347-7.00028-8>
- Wang, J.-G. 2016 . Engineering Nanostructured MnO<sub>2</sub> for High Performance Supercapacitors. In *Supercapacitor Design and Applications*. InTech. <https://doi.org/10.5772/65008>
- Zhang, F., Zhang, T., Yang, X., Zhang, L., Leng, K., Huang, Y., & Chen, Y. 2013 . A High-Performance Supercapacitor-Battery Hybrid Energy Storage Device Based on Graphene-Enhanced Electrode Materials with Ultrahigh Energy Density. *Energy and Environmental Science*, 6(6), 1623–1632. <https://doi.org/10.1039/c3ee40509e>
- Zhang, H., Gu, J., Jiang, Y., Wang, Y., Zhao, J., Zhang, X., & Wang, C. 2014 . Calcination Removing Soft Template Cetyl Trimethyl Ammonium Bromide and Its Effects on Capacitance Performance of Supercapacitor Electrode MnO<sub>2</sub>. *Energy Conversion and Management*, 86, 605–613. <https://doi.org/10.1016/j.enconman.2014.06.039>
- Zhao, X., Hou, Y., Wang, Y., Yang, L., Zhu, L., Cao, R., & Sha, Z. 2017 . Prepared MnO<sub>2</sub> with Different Crystal Forms as Electrode Materials for Supercapacitors: Experimental Research from Hydrothermal Crystallization Process to Electrochemical Performances. *RSC Advances*, 7(64), 40286–40294. <https://doi.org/10.1039/c7ra06369e>